

## EXPERIMENTAL ANALYSES IN STATIC REGIME ON THE REDUCED SCALE MODEL OF THE STRUCTURE OF THE DOUBLE BOTTOM

**Anișoara - Gabriela Cristea**  
"Dunarea de Jos" University of Galati,  
Faculty of Naval Architecture, Galati,  
Domneasca Street, No. 47, 800008, Romania,  
E-mail: [anișoara.cristea@ugal.ro](mailto:anișoara.cristea@ugal.ro)

### ABSTRACT

*The purpose of this paper consists in the experimental analyses in static regime on the reduced scale model of the structure of double bottom. For modelling and stress analysis around relief cutting of a frame floor, the program system with SolidWorks / COSMOS/M finite element was used. In order to validate the results of numerical modelling it was designed an experimental modelling program. This program contained several kinds of experimental modelling: using Resistive Electric Tensometry (RET) and Optical Method (OM) method. A stand was designed to carry out on an experimental checking of the variation of the stress status in the Experimental Model reduced to scale of 1:10.*

**Keywords:** finite element method, deformations, static analysis, stress concentration, normal stress, Resistive Electric Tensometry (RET) and Optical Method (OM)

### 1. INTRODUCTION

The study of this paper concerns a vessel used to transport chemical compounds (chemical tanker) of 8000 tdw (Figure 1). All references to naval structures have this vessel as target. The most reinforced framework from the double bottom and which therefore presents a real interest is represented by frame floor. In general, these have technological cuttings for the passage of piping from ballast installation – bilge, cable routes. These cuttings, usually rectangular, are the hot-spots stress areas due to their corner shape. For modelling and stress analysis around relief cutting of a frame floor, the program system with SolidWorks / COSMOS/M finite element was used. The structure taken into structure in this paper is that of a chemical tanker 8000 tdw. This type of vessel is built in framework longitudinal system. Its main sizes are presented in the table below (Table 1).

Using Germanischer Lloyd, Poseidon program, for the chemical tanker studied in this paper, the preliminary structural model was made, in accordance with the local and general resistance rules. The cross-section through this vessel is presented in Fig 1.

The material used is AH36 naval steel, its characteristics being presented in Table 1.

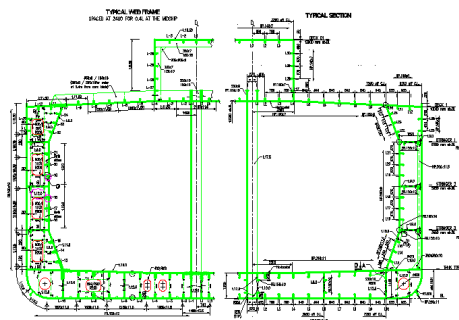


**Fig. 1** The cross-section to the chief frame through the real size vessel

**Table 1** Geometrical and material characteristics for double bottom structure

|  |                            |
|--|----------------------------|
| The overall length of the vessel, $L_{OA}$ | 118.160 m                  |
| Length between perpendiculars, $L_{pp}$    | 110.596 m                  |
| Width of vessel, $B$                       | 18.500 m                   |
| Full load draft, $T$                       | 7.400 m                    |
| Height of construction, $D$                | 10.000 m                   |
| Block coefficient, $C_B$                   | 0.730                      |
| Vessel speed in calm water, $v$            | 14 knots                   |
| Displacement, $\Delta$                     | 8000 tdw                   |
| Young's modulus, $E$                       | 2.1E+5 MPa                 |
| Poisson coefficient, $\nu$                 | 0.3                        |
| The density of steel, $\rho$               | 7.85E-6 kg/mm <sup>3</sup> |
| Yield strength, $R_{eH}$                   | 355 MPa                    |
| Tensile strength, $R_m$                    | 360 - 480 MPa              |

There is symmetry to Diametral Plane (DP) so that only half of the model will be considered for analysis (Fig. 2).

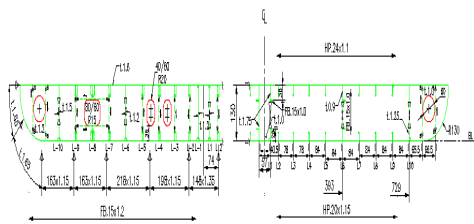


**Fig. 2** Structure of double bottom for reduced scale model

In order to determine the status of stress in the structures, many analytical and numerical methods are used.

A classification of numerical modelling methods can be made from the mathematical point of view (mathematical modelling of various problems of mechanics being independent of the physical nature of these problems) on three main directions: Finite Difference Method, Finite Element Method and Boundary Element Method.

The structure was found to be recessed at one end and free at the other end. The loading was done on the free end through a uniformly distributed load. The finite elements used were quadrilaterals membrane and thick plate shell elements. A number of 22464 elements and 22621 knots resulted from meshing. The structure meshing is shown in Fig 3.

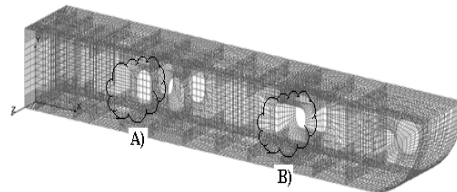


**Fig. 3** Meshing by finite elements of reduced scale model structure

Numerical models were made for double-bottom structures with connection radius of cut-hols 15, 20, 25 mm (at real size vessel the radius was 150, 200, 250 mm). The loading of structure was made on coupling area of bilge with double-bottom sheet and had as values 2.5, 5, 7.5 kN respectively. The structure links are in the area of the Diametral Plane (DP) of the vessel. This link was chosen because of the symmetry of double-bottom structure to DP.

As only an area that included an inter-course distance in the knots from the edge of the modelled structure was analyzed, the spins after axes Oy were blocked.

In order to perform comparative analyses, two cuttings from the area of double-bottom were considered. These cuttings may be seen in Figure 4 (meshing by finite elements).

Choosing these cuttings was dictated by technical considerations. Thus:

- in the area of cutting noted with A), tensometric marks were placed and measurements were made using Resistive Electric Tensometry (RET) method. This area was also analysed using Optical Method (OM).

- in the area of cutting noted with B), the detection of stress concentrations was performed and the crack initiation was made.

There were selected the hot-spots stress area where the structural response was analyzed, as follows:

- Figure 4a) in order to perform validation of numerical results with experimental results obtained by RET and OM in the area of elastic strain of materials;

- Figure 4b) in order to validate the numerical results with experimental results obtained by OM for the elasto - plastic strain area of materials.

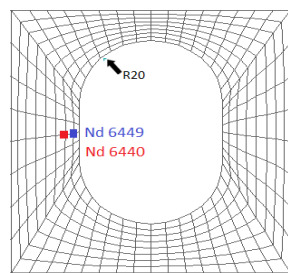


**Fig. 4 a)** Distribution of analysed knots

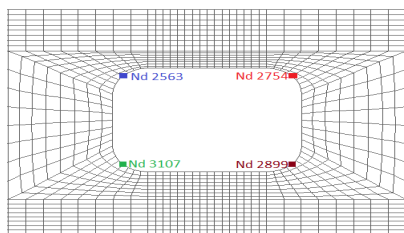


**Fig. 4 b)** Distribution of analysed knots

In order to validate the results of numerical modelling, it has been designed an experimental modelling program. This program contained several kinds of experimental modelling: using Resistive Electric Tensometry (RET) and Optical Method (OM) method. A stand was designed to carry out on an experimental checking of the variation of the stress status in the Experimental Model reduced to scale of 1:10. The thickness of tablets was of

1.2 mm. Thus three experimental models were built having connection radii of different technological cuttings.

The performed Experimental Model is presented in Figure 5. In Figure 5a) the three executed experimental methods are presented, with previous mentioned radii of connection. In Figure 5b) the experimental stand is presented and consists in:

- double bottom structure reduced to scale 1:10;

- rigid clamping frame structure and charging system;

- system of executing the strain cargo consisting of: screw with two beginnings, system of rigid clamping frame structure, dynamometers for measuring the cargo;

- stress measurement tensometric system consisting of: strain gauges with strain transducers with measurement basis of 10 mm and own ohmic resistance of 120  $\Omega$ , applied on the part opposite the optical measurement system (Figure 6), cables, Spider 8 tensometric bridge and laptop with Catman Express 3.1 software for recording the data of measurements;

- ARAMIS HS optical measurement system produced by GOM German company – where the method itself is based on the comparison of distances between landmarks in various stages of strain. Due to occurrence of performant computers and certain computer programs for the study, the transformation of optical effects in digital signals was possible, giving information about the strain status at the surface of structures. The equipment is in the laboratory of Material Resistance within the Faculty of Naval Architecture of 'Dunarea de Jos' University of Galati.

ARAMIS HS System uses the latest techniques for optical measurements of three-dimensional deformation and of specific deformations.

The advantage of the method is that the material is not influenced in structure, being a non-destructive method.

The value differences obtained through Experimental Method, compared with Nu-

merical Method, indicates the fact that measurement errors were due to model errors (caused by model imperfections related to measured) and instrument errors (caused by measurement instruments). Using this equipment, it was noticed that the measurement uncertainty lies between reasonable values.

Due to small thicknesses of component tables, the Experimental Model could not be continuously welded. Therefore at the reduced scale model, used also for experimental modelling, the weldings were discontinuous. The numerical analyses performed on this reduced model took into account this detail.

Analyses were made taking into account double bottom reduced scale structure welded continuously and discontinuously.

The strain gauges were applied in the area of 6449 and 6440 knots, Fig. 6, where tables and results of numerical calculations were performed.



Fig. 5 a) Achieved experimental model



Fig. 5 b) Achieved experimental model



Fig. 6 Location of strain gauges

## 2. MODELINGS USING RESISTIVE ELECTRIC TENSOMETRY METHOD

Within these experiments, Experimental Model was statically loaded with loads applied on the 'open end of structure'. The application of load was made through a screw with two beginnings, progressively, from 0 to maximum value of 7.5 kN. The record of deformations was made for only for values 0, 2.5, 5.0, 7.5 kN. These deformations were further processed and stresses resulted in the areas of location of strain gauges.

The results obtained by processing of tensometric measurements results are presented in Table 1.

Table 2 Tensometric measured stress for area of elastic strain of materials

| Knot<br>(Fig. 4a) | Force<br>(kN) | Von Mises Stress (MPa)    |       |       |
|-------------------|---------------|---------------------------|-------|-------|
|                   |               | Radius of connection (mm) |       |       |
|                   |               | 15                        | 20    | 25    |
| 6440              | 2.5           | 3.835                     | 3.812 | 3.807 |
| 6449              |               | 2.120                     | 2.110 | 2.101 |
| 6440              | 5             | 7.725                     | 7.745 | 7.710 |
| 6449              |               | 4.289                     | 4.208 | 4.108 |

|      |     |        |        |        |
|------|-----|--------|--------|--------|
| 6440 |     | 12.163 | 12.011 | 11.985 |
| 6449 | 7.5 | 6.469  | 6.326  | 6.301  |

For measurement of their vertical displacements a comparator clock was used. Thus the displacements of interest points have resulted in Table 2.

Before performing experiments, the maximum load was calculated so that the strains may be considered in elastic domain. The displacements of cross sections during strain from 0 to 7.5 kN may be also considered as occurring in this field. Hence, it can be concluded that cross sections behave as if they were rigid. For measurement of their vertical displacements, a comparator clock was used. Thus the displacements of interest points have resulted in Table 3.

**Table 3** Measured displacements using TER

| Knot<br>(Fig. 4a) | Force<br>(kN) | Von Mises Stress (MPa)    |      |      |
|-------------------|---------------|---------------------------|------|------|
|                   |               | Radius of connection (mm) |      |      |
|                   |               | 15                        | 20   | 25   |
| 6440              | 2.5           | 0.06                      | 0.06 | 0.05 |
| 6449              |               | 0.05                      | 0.06 | 0.05 |
| 6440              | 5             | 0.11                      | 0.10 | 0.11 |
| 6449              |               | 0.11                      | 0.11 | 0.11 |
| 6440              | 7.5           | 0.17                      | 0.17 | 0.16 |
| 6449              |               | 0.17                      | 0.17 | 0.16 |

### 3. MODELINGS USING OPTICAL METHODS (OM) LOADING THE STRUCTURE

The main components of optical measurement system are (Figure 7):

- ❖ sensor with 2 cameras (2);
- ❖ calibration objects;
- ❖ device for cameras operation and control of the recorded images (1);
- ❖ computing system with data acquisition (1);
- ❖ additional lighting system, local (3);
- ❖ Linux operating system and ARAMIS HS software application.

The stages of an experiment using OM are:

- A. preparation of cameras
  - i. adjustment of distances and angles between cameras;

- ii. adjustment of distance between cameras and model;
- iii. adjustment of luminosity of cameras;
- iv. focalization of cameras.

Calibration of cameras

This is made, depending on the type of experiment using 'calibration crosses' or 'artifacts', Fig. 8 a, b.



**Fig. 7)** Components of ARAMIS HS optical measurement system



**Fig. 8a)** Calibration equipment – Calibration crosses



**Fig. 8b)** Calibration equipment - Artifacts

The measurements through OM consist in recording distance variation between defined points, after loads. The record of data is made during all process of loading, thus the obtained data are saved per stages (data being recorded at a rate of sampling preset by soft used at 0.01 sec). The status of deformation in the studied area has resulted in the analysis of these data per stages.

In the images below, graphics of variation of displacements for 3 radii of connection are presented. These results are presented for the 3 radii of connection. These results are presented for loading capacities of 2.5, 5.0, 7.5 kN (Table 4).

A special effort was involved in choosing the appropriate stage, through the identification of purchased data corresponding to interest capacity. This thing was achieved by recording the time of experiment duration.

**Table 4** Measured displacements using TER

| Knot<br>(Fig. 4a) | Force<br>(kN) | Von Mises Stress (MPa)    |       |        |
|-------------------|---------------|---------------------------|-------|--------|
|                   |               | Radius of connection (mm) |       |        |
|                   |               | 15                        | 20    | 25     |
| 6440              | 2.5           | 0.057                     | 0.054 | 0.051  |
| 6449              |               | 0.056                     | 0.055 | 0.053  |
| 6440              | 5             | 0.110                     | 0.109 | 0.109  |
| 6449              |               | 0.113                     | 0.111 | 0.1113 |
| 6440              | 7.5           | 0.159                     | 0.164 | 0.169  |
| 6449              |               | 0.160                     | 0.167 | 0.171  |

**4. CONCLUSIONS**

In order to conclude upon the methodology of addressing the issues of behaviour of double bottom structure in the area of technological cuttings under loads, data obtained by calculation and experimental measurements for reduced scale model are centralized in Table 5.

As it can be seen, the numerical results are well checked experimentally. The differences resulted in the analysis of tabulated data are insignificant.

Since, as previously stated, the experimental model could not be welded continuously, due to small thicknesses of components, reason for which an analysis of stresses

for the case of continuous welds (CW) and discontinuous welds (DW) should be made.

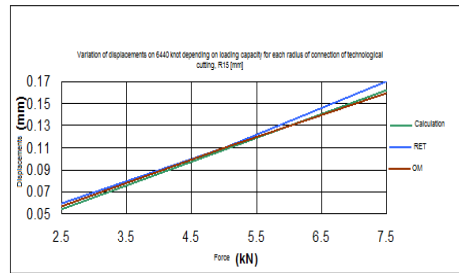


**Fig. 9 a)** Variation of displacements on 6440 knot depending on loading capacity for each radius of connection of technological cutting (R15)

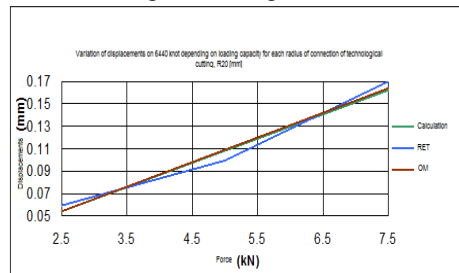


**Fig. 9 b)** Variation of displacements on 6440 knot depending on loading capacity for each radius of connection of technological cutting (R20)

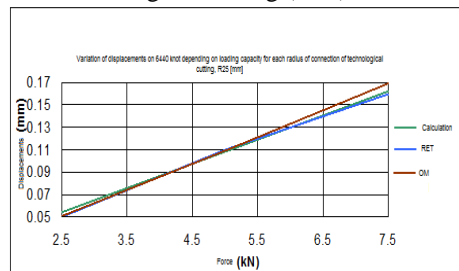


**Fig. 9 c)** Variation of displacements on 6440 knot depending on loading capacity for each radius of connection of technological cutting (R25)

Using a graphical representation of variation of stress (Fig. 11, 12) it can be seen that differences are really insignificant. The maximum value of differences is of 7%.

Centralizing data in Table 6, it can be seen that there are no significant differences

between the two welding methods used to achieve reduced scale model (experimental).

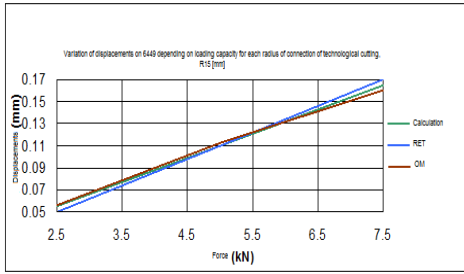


**Fig. 10 a)** Variation of displacements on 6449 depending on loading capacity for each radius of connection of technological cutting (R15)

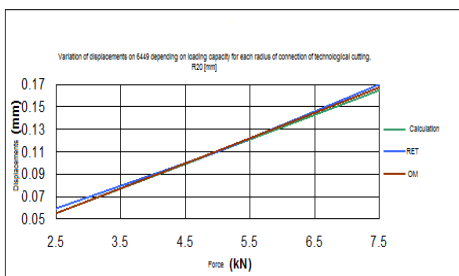


**Fig. 10 b)** Variation of displacements on 6449 depending on loading capacity for each radius of connection of technological cutting (R20)

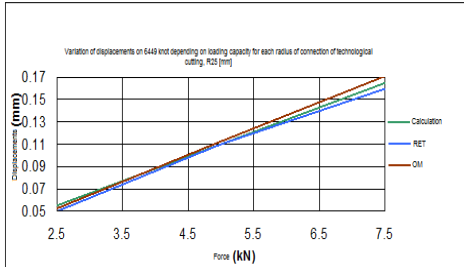


**Fig. 10 c)** Variation of displacements on 6449 depending on loading capacity for each radius of connection of technological cutting (R25)

The important conclusion which results from studies made is that the designed methodology may be used for further studies of this paper. Based on the data validation by experimental

tests that lead to adoption of methodology designed for numerical analysis of real size vessel.

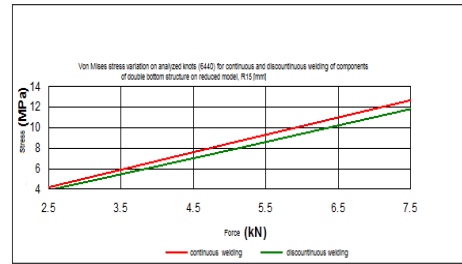


**Fig. 11)** Von Mises stress variation on analyzed knots for continuous and discontinuous welding of components of double bottom structure on reduced model

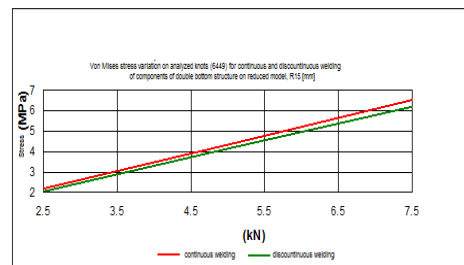


**Fig. 12)** Von Mises stress variation on analyzed knots for continuous and discontinuous welding of components of double bottom structure on reduced model

**REFERENCES**

- [1]. **Domnişoru L.**, "Analiza structurilor navale prin metoda elementului finit. Aplicatii numerice", Editura Fundației Universitare "Dunărea de Jos", Galați, 2009.
- [2]. **Domnişoru L., Găvan E., Popovici O.**, "Analiza structurilor navale prin metoda elementului finit", Editura Didactica și Pedagogică, București, 2005.
- [3]. **Cristea A.**, *Contribuții privind optimizarea structurilor de navă*, Teză de doctorat, Galați, 2014.
- [4]. **Hadăr A., Constantinescu I.N., Gheorghiu H., Coteș C.E.**, *Modeling and models for calculations in mechanical engineering*, PRINTECH Publishing House, Bucharest, 2007.
- [5]. **x x x – Documentație SolidWorks / COSMOS/M**
- [6]. **x x x – SolidWorks / COSMOS/M**

| Knot<br>(Fig. 4 a) | Force<br>(kN) | Displacements (mm)        |      |       |             |      |       |             |      |       |
|--------------------|---------------|---------------------------|------|-------|-------------|------|-------|-------------|------|-------|
|                    |               | Radius of connection (mm) |      |       |             |      |       |             |      |       |
|                    |               | 15                        |      |       | 20          |      |       | 25          |      |       |
|                    |               | Calculation               | RET  | OM    | Calculation | RET  | OM    | Calculation | RET  | OM    |
| 6440               | 2.5           | 0.0542                    | 0.06 | 0.057 | 0.0542      | 0.06 | 0.054 | 0.0542      | 0.05 | 0.051 |
| 6449               |               | 0.0549                    | 0.05 | 0.056 | 0.0549      | 0.06 | 0.055 | 0.0549      | 0.05 | 0.053 |
| 6440               | 5.0           | 0.1083                    | 0.11 | 0.110 | 0.1083      | 0.10 | 0.109 | 0.1083      | 0.11 | 0.109 |
| 6449               |               | 0.1097                    | 0.11 | 0.113 | 0.1097      | 0.11 | 0.111 | 0.1097      | 0.11 | 0.113 |
| 6440               | 7.5           | 0.1625                    | 0.17 | 0.159 | 0.1625      | 0.17 | 0.164 | 0.1625      | 0.16 | 0.169 |
| 6449               |               | 0.1646                    | 0.17 | 0.160 | 0.1646      | 0.17 | 0.167 | 0.1646      | 0.16 | 0.171 |

| Knot<br>(Fig. 4 a) | Force<br>(kN) | Von Mises Stress (MPa)    |       |       |       |       |       |
|--------------------|---------------|---------------------------|-------|-------|-------|-------|-------|
|                    |               | Radius of connection (mm) |       |       |       |       |       |
|                    |               | 15                        |       | 20    |       | 25    |       |
|                    |               | SC                        | SD    | SC    | SD    | SC    | SD    |
| 6440               | 2.5           | 4.22                      | 3.927 | 4.22  | 3.927 | 4.22  | 3.927 |
| 6449               |               | 2.178                     | 2.069 | 2.178 | 2.069 | 2.178 | 2.069 |
| 6440               | 5.0           | 8.441                     | 7.854 | 8.441 | 7.854 | 8.441 | 7.854 |
| 6449               |               | 4.355                     | 4.138 | 4.355 | 4.138 | 4.355 | 4.138 |
| 6440               | 7.5           | 12.66                     | 11.78 | 12.66 | 11.78 | 12.66 | 11.78 |
| 6449               |               | 6.533                     | 6.207 | 6.533 | 6.207 | 6.533 | 6.207 |

*Paper received on December 20<sup>th</sup>, 2016*